THE PENNSYLVANIA STATE UNIVERSITY
SCHREYER HONORS COLLEGE

DEPARTMENT OF ENGINEERING SCIENCE AND MECHANICS

BIOMECHANICAL MODELLING OF BIOLOGICAL TISSUES:
IMPORTANCE TO TUMOR CLASSISIFICATION

ANTONY J. PALOCAREN

Spring 2010

A thesis
submitted in partial fulfillment
of the requirements
for a baccalaureate degree
in Engineering Science
with honors in Engineering Science

Reviewed and approved* by the following:

Dr. Corina Drapaca
Assistant Professor of Engineering Science and Mechanics
Thesis Adviser

Dr. Joseph L. Rose
Professor of Engineering Science and Mechanics
Honors Adviser

Judith A. Todd
P. B. Breneman Deparment Head Chair
Professor, Department of Engineering Science and Mechanics

Signatures are on file in the Schreyer Honors College and Engineering Science and Mechanics Office.

ABSTRACT

Biological tissues possess viscoelastic features, *i.e*. they have rigid characteristics as like solids, but also dissipate energy just as viscous fluids. Diseases change the mechanical properties of biological tissues. These changes of mechanical properties are caused either by the seepage of fluids into the intercellular space or by the loss of lymphatic fluids, as in the case of cancer. The result is usually an increase in stiffness or elastic modulus of the pathologic tissue. None of the modern, non-invasive, imaging techniques (such as CT, MR or Ultrasound Imaging) used today by clinicians to find and diagnose tumors, provide the critical information about the stiffness of the imaged tissues. In recent years a lot of progress has been made in implementing information about the Young's modulus of tissues into the clinical imaging techniques. However, the biomechanical models used to find Young's moduli of tissues fail to differentiate not only between normal and abnormal tissues but, more importantly, between benign and malignant (cancer) tumors. In this thesis we present a novel biomechanical model that uses information from image mass spectroscopy of tissues to classify low grade (benign) and high grade (malignant) gliomas based on the difference between their Young's moduli. We also propose a new growth model for tumors that is dependent on the mechanical properties of tissues.

ACKNOWLEDGEMENTS

TABLE OF CONTENTS

Chapter 1

Introduction

For centuries, palpation has been an important medical diagnostic tool. The efficacy of palpation is based on the fact that many diseases can change the mechanical properties of tissues. These changes are caused either by the exudation of fluids from the vascular into the extra- and intercellular space or by loss of lymphatic systems, as in the case of cancer. The result is an increase in stiffness or elastic modulus of the tissue. To this day, health professionals try to feel for lesions during surgery that have been missed by a CAT scan, ultrasound or magnetic resonance. None of these scans can provide the information about the elastic properties of tissue elicited by palpitation. The elastic moduli of various human soft tissues are known to vary over a wide range, more than four orders of magnitude. In contrast, most of the physical properties depicted by conventional medical imaging modalities are distributed over a much smaller numerical range. These observations have provided the motivation for many researchers to seek medical imaging technology that can estimate or assess the elastic moduli of tissues. The approaches to date have been to use conventional imaging methods to measure the mechanical response of tissue to mechanical stress. The resulting strains have been measured using ultrasound, CT, or MRI and the related elastic modulus has been computed from biomechanical models of tissues. In particular, the MR elastography method (MRE) using harmonic shear waves offers direct visualization and quantitative measurement of tissue displacements, high sensitivity to very small motions, a field of view unencumbered by acoustic window requirements, and the ability to obtain full three dimensional displacement information throughout a volume.

In order to recover the mechanical properties of biological tissues we need to invert the displacement data measured by the MRE method. This inversion process requires the use of an

accurate biomechanical model for tissues. It was noticed experimentally that most biological tissues have incompressible viscoelastic features: they have a certain amount of rigidity that is characteristic of solid bodies, but, at the same time, they flow and dissipate energy by frictional losses as viscous fluids do. The incompressibility assumption for soft tissues is based on the fact that most tissues are made primarily of water. In addition, since the displacements in MRE are very small (on the order of microns), a linear constitutive law is usually assumed. However, despite the richness of the data set, the variety of processing techniques and simplifications made in the biomechanical model, it remains a challenge to extract accurate results at high resolution in complex, heterogeneous tissues from the intrinsically noisy data. Therefore, any improvement in the MRE data processing with the help of biomechanics and computational methods will be of significant importance to modern medicine. MRE can help in tumor detection, determination of characteristics of disease, and in the assessment of rehabilitation.

The aim of this thesis is to formulate new biomechanical models that will be able to differentiate not only between normal and abnormal tissues, but may be more importantly, between benign and malignant tumors. As it can be seen in Fig.1, benign tumors tend to be more isotropic, and look more regularly shaped due in part to the presence of fibrous connective tissue shells that separate the benign tumors from the surrounding healthy tissue. On the other hand, malignant tumors are diffusive, anisotropic and irregularly shaped.

In order for the MRE method to correctly classify tumors in benign and malignant, the constitutive models of these two classes of tumors need to incorporate the biochemical differences between them. We believe that a more accurate formulation of the direct problem of MRE will help us not only to gain a better understanding of the tumors' biomechanics but also to obtain more reliable elastic moduli by solving the inverse problem. The aim of this thesis is to link the mechanical and biochemical properties of biological tissues, and thus this research lies at

the frontiers between engineering science and mechanics and medicine (more precisely, diagnostic radiology).
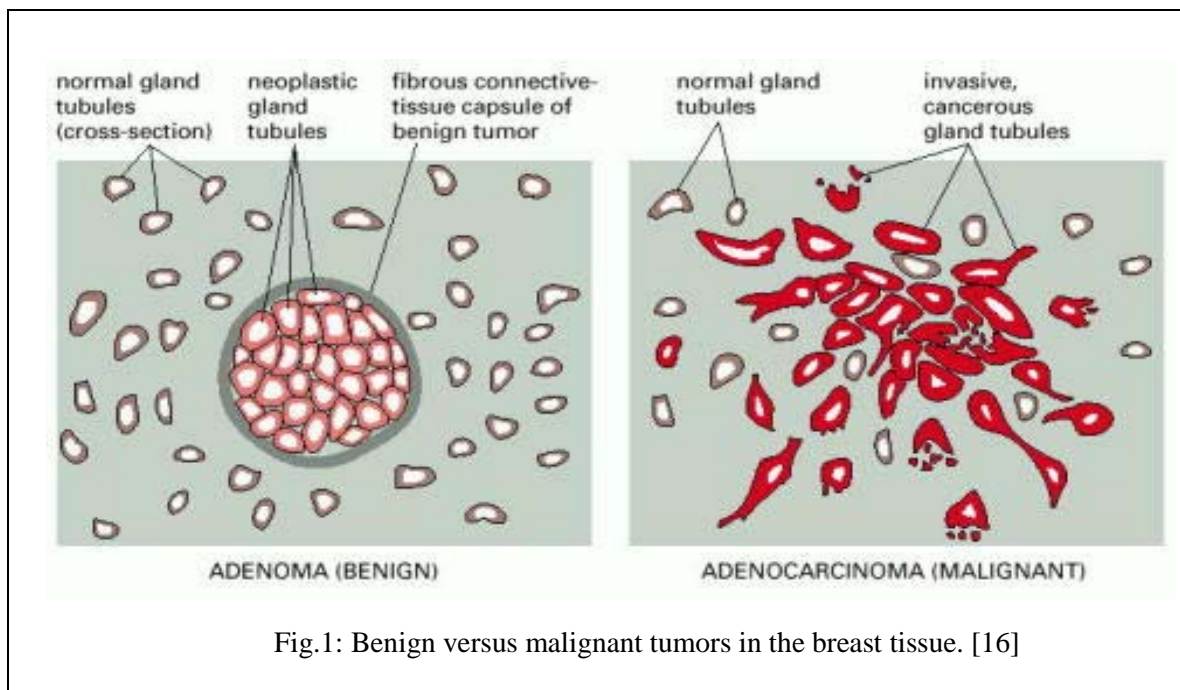

Fig.1: Benign versus malignant tumors in the breast tissue. [16]

In this thesis we propose a novel biomechanical model for the Young's moduli of tumors that depend on the mass spectra of the proteins present in the tissues. We will show that the Young's modulus of high grade glioma is at least 10kPa higher than the Young's modulus of a low grade glioma. In addition, we also investigate the effect of mechanics on the growth of tumors. The prediction of tumor growth is essential in treatment decision and planning.

Understanding the relationship between the mechanics and the biochemistry of biological tissues will have a tremendous impact on the development of advanced diagnostic and treatment clinical procedures. This work has the potential to play an important role in developing better non-invasive imaging techniques capable not only to find but also to properly classify tumors, thus drastically reducing both - the very high health-related costs for medical diagnosis and treatments (economic component) and the number of deaths due to wrong diagnosis or delayed treatment (social component).

Chapter 2

Literature Review

In this chapter we review the mass spectroscopy and magnetic resonance techniques, as well as the clinical classification of tumors using grades.

Mass Spectroscopy

Mass spectroscopy is one of the most accurate methods for determining the elemental composition of a substance or a molecule. The primary principle for this method is to ionize the substance or the chemical compound by bombarding it with high energy electrons (Fig. 2). As a result, positively charged fragments are produced and are accelerated in a vacuum through a magnetic field and are sorted on the basis of mass to charge ratio. Since the bulk of the ions produced in the mass spectrometer carry a unit positive charge, the value m/e is equivalent to the molecular weight of the fragment. We use this feature of mass spectroscopy to relate the Young's Modulus to the concentration of proteins in the tissue. Tissue mass spectral analysis can be carried out through either a profiling or imaging approach. In the profiling approach, only specific locations within the tissue section are analyzed. In the imaging approach, protein distributions can be visualized over the entire tissue section.

In recent years, mass spectrometry has become an indispensable tool for proteomic studies [1]. Desorption and ionization techniques such as matrix-assisted laser desorption ionization mass spectrometry (MALDI MS) and electrospray ionization mass spectrometry (ESI MS) have literally revolutionized our ability to analyze proteins. These improvements offer levels of sensitivity and mass accuracy never before achieved for the detection, identification and structural characterization of proteins. It is now possible to routinely measure molecular weights

above 200 kDa as well as obtain low parts per million mass measurement accuracies for the determination of peptides and proteins. Protein identification has been greatly facilitated because of the rapid expansion of protein and gene databases. Modern mass spectrometers can now rapidly map and fragment peptides that result from protease digestion in order to obtain sequence information and identify proteins [2]. MALDI MS is an ideal tool to investigate complex protein mixtures. It utilizes a matrix, a small acidic aromatic molecule that absorbs energy at the wavelength of the irradiating laser. The analyte molecule is mixed with the matrix in a ratio of typically 1/5000, deposited on a target plate and allowed to dry. During the drying process, matrix-analyte cocrystals form. These crystals are then submitted to very short laser pulses (typically UV laser light), resulting in desorption and ionization of the analyte molecule. Mostly intact protonated molecular ions are formed ([M+H], where M is the molecular weight of the analyte molecule). The mass-to-charge (m/z) of the ion is typically measured in a time-of flight mass analyzer (Fig.3) [3].

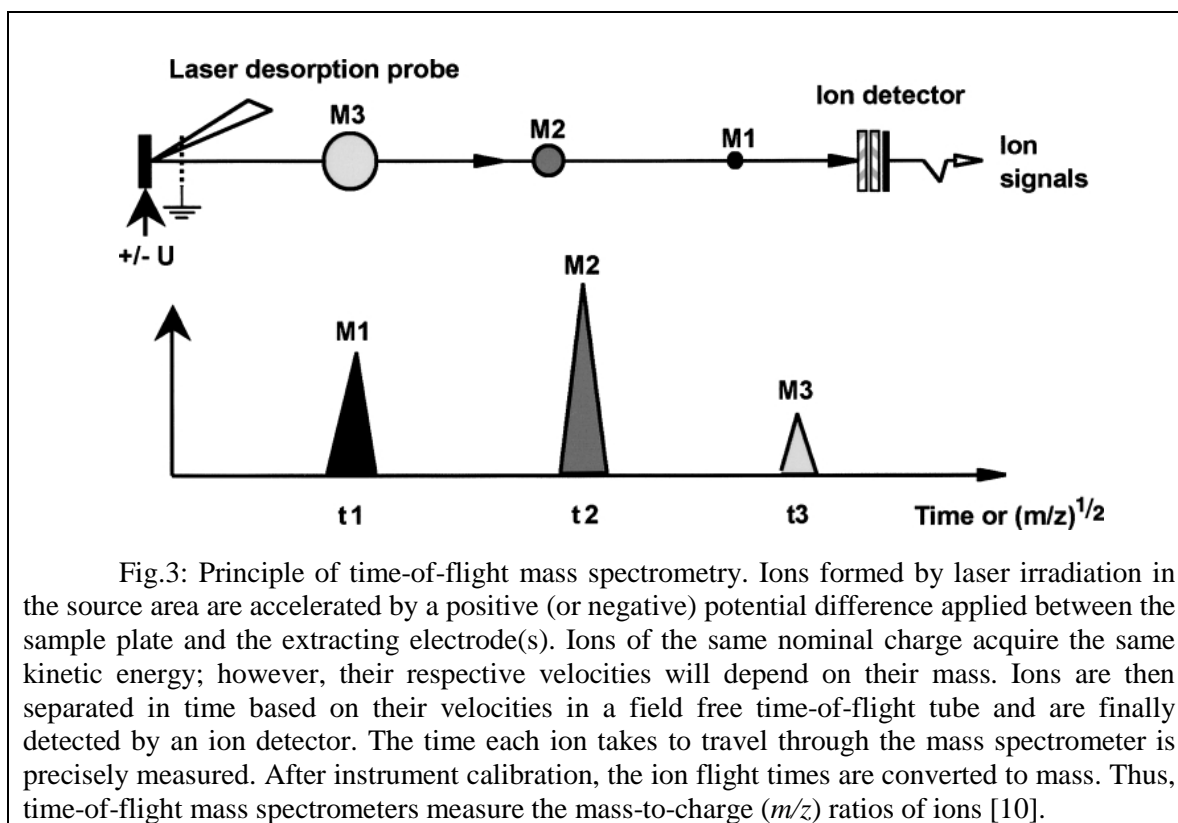Fig.2: Classic mass spectroscopy setup [17]
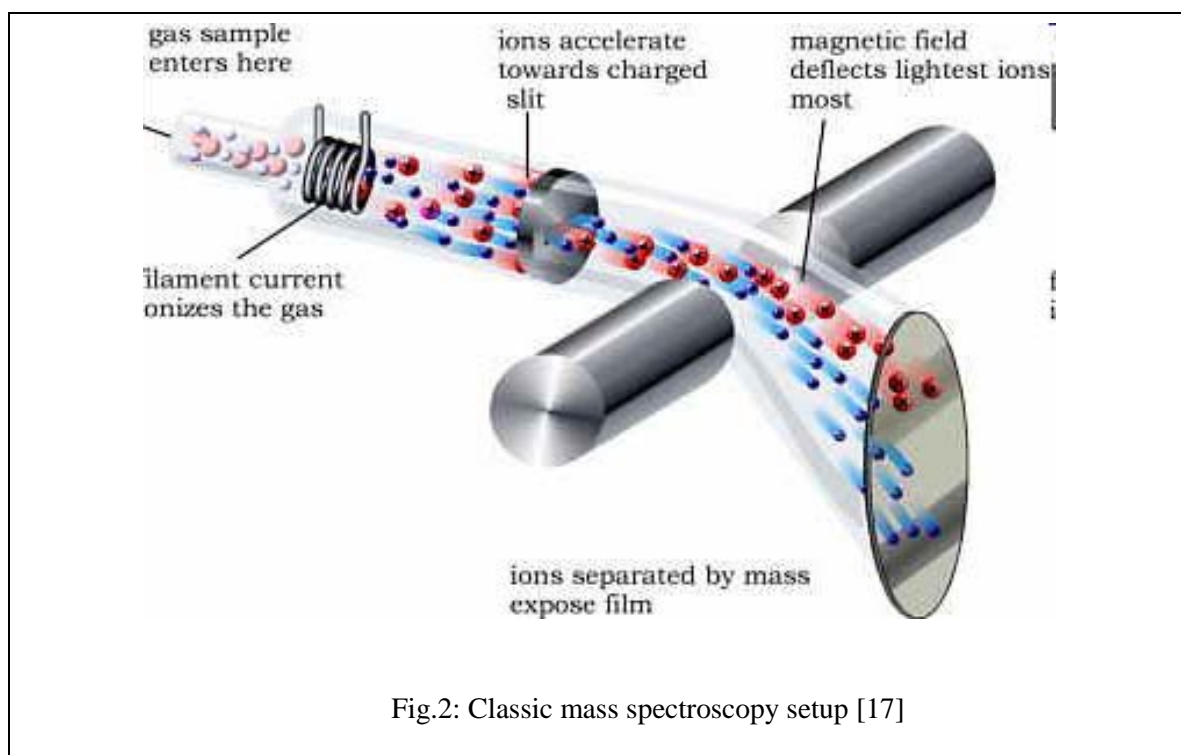
Fig.3: Principle of time-of-flight mass spectrometry. Ions formed by laser irradiation in the source area are accelerated by a positive (or negative) potential difference applied between the sample plate and the extracting electrode(s). Ions of the same nominal charge acquire the same kinetic energy; however, their respective velocities will depend on their mass. Ions are then separated in time based on their velocities in a field free time-of-flight tube and are finally detected by an ion detector. The time each ion takes to travel through the mass spectrometer is precisely measured. After instrument calibration, the ion flight times are converted to mass. Thus, time-of-flight mass spectrometers measure the mass-to-charge (*m/z*) ratios of ions [10].

One of the recent applications of MALDI MS is its use to profile and image proteins directly from thin tissue sections. MALDI imaging mass spectrometry (IMS) is a new technology that allows for simultaneous mapping of hundreds of peptides and proteins present in thin tissue sections with a lateral resolution of about 30–50 μm. Matrix is first uniformly deposited over the surface of the section, utilizing procedures optimized to minimize protein migration. Proteins are then desorbed from discrete spots or pixels upon irradiation of the sample in an ordered array or raster of the surface. Each pixel thus is keyed to a full mass spectrum consisting of signals from protonated species of molecules desorbed from that tissue region. A plot of the intensity of any one signal produces a map of the relative amount of that compound over the entire imaged surface. This technology provides an extremely powerful discovery tool for the investigation of biological processes [4, 5, 6, 7, 10].

Direct tissue mass spectral analysis can be carried out through either a "profiling" or an "imaging" approach. In the profiling approach, only specific locations within the tissue section are analyzed often correlated with classical histology. In the imaging approach, protein distributions can be visualized over the entire tissue section. These processes are illustrated in Fig. 4. In the profiling approach, matrix is deposited in discrete locations according to cell type to be analyzed across the tissue section, (Fig. 4A), and distinct mass spectra are obtained from each matrix spot (Fig. 4B). In the imaging approach, the matrix is deposited robotically in an array or uniformly coated across the tissue section, (Fig. 4C) and mass spectra are acquired systematically and are reconstructed into 2-D false color ion-density images (Fig. 4D).

Fig. 4: Profiling *versus* IMS demonstrated on human breast cancer tissue [18].
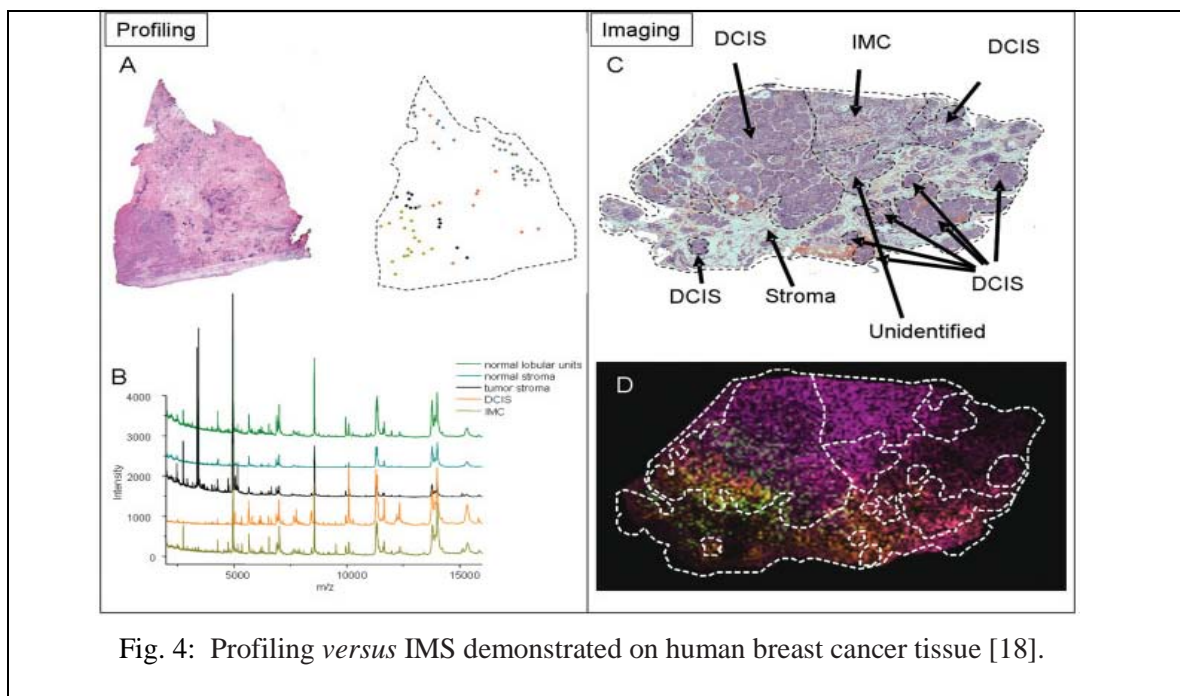
The result of the profiling mass spectroscopy is a plot of the relative concentration (intensity) of the proteins found in the tissue versus the mass-to-charge ratio. Image mass spectroscopy gives a map of the proteins' densities in the tissue. A schematic diagram of the general experimental procedure described above is given in Fig.5.
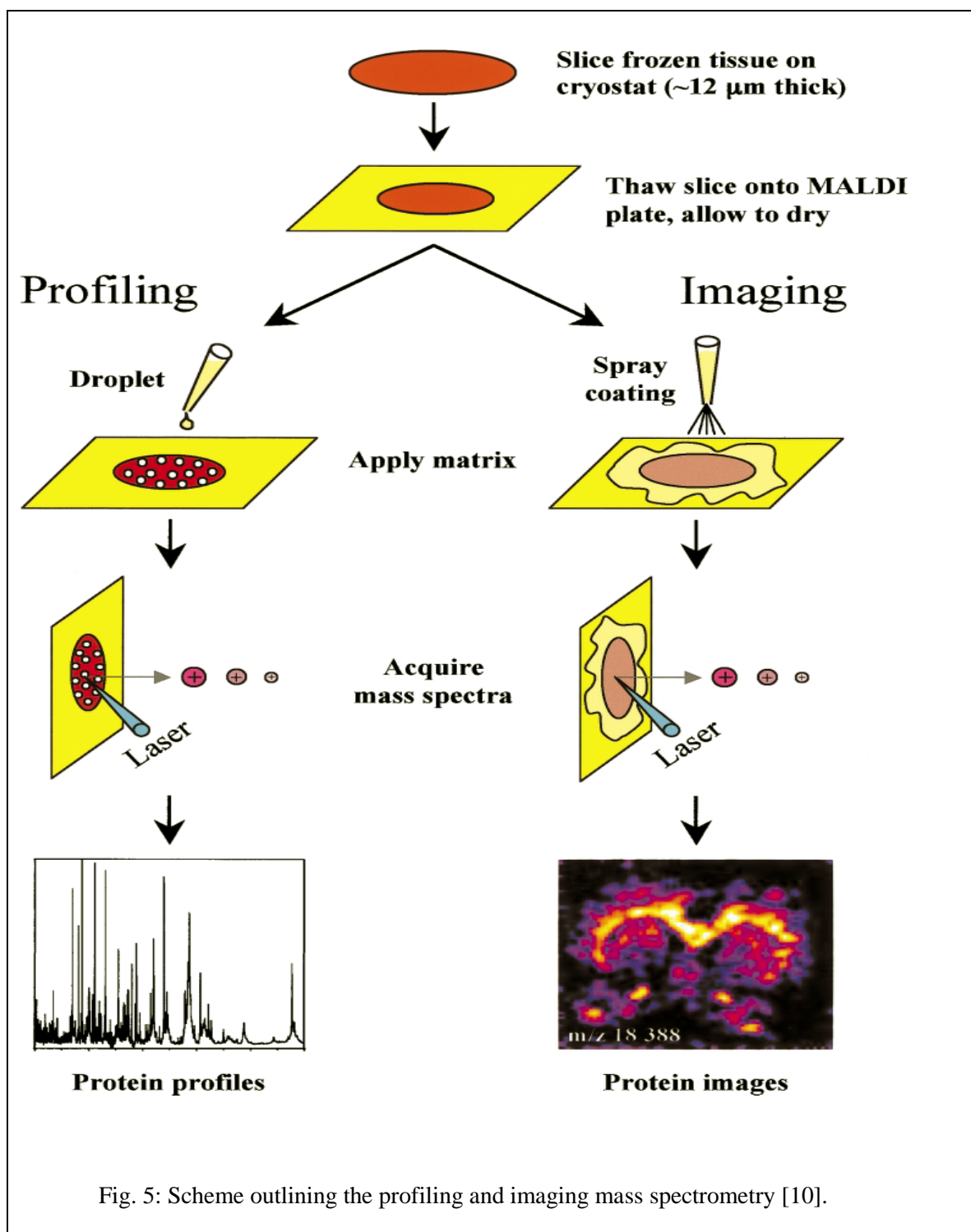
Fig. 5: Scheme outlining the profiling and imaging mass spectrometry [10].

Tumor Grading

Tumor grade is a system used to classify cancer cells in terms of how abnormal they look under a microscope and how quickly the tumor is likely to grow and spread. Histological grade, also called differentiation, refers to how much the tumor cells resemble normal cells of the same tissue type. Nuclear grade refers to the size and shape of the nucleus in tumor cells and the percentage of tumor cells that are dividing [11].

Based on the microscopic appearance of cancer cells, pathologists commonly describe tumor grade by four degrees of severity: Grades 1, 2, 3, and 4. Cells of Grade 1 resemble normal cells, and tend to grow and multiply slowly. Grade 1 tumors are generally considered the least aggressive in behavior. However, cells of Grade 3 or Grade 4 do not look like normal cells of the same type. Grade 3 and 4 tumors tend to grow rapidly and spread faster than tumors with a lower grade. The American Joint Commission on Cancer recommends the following guidelines for grading tumors shown in table 1.

| Grade	Description
GX	Grade cannot be assessed (Undetermined grade)
G1	Well-differentiated (Low grade)
G2	Moderately differentiated (Intermediate grade)
G3	Poorly differentiated (High grade)
G4	Undifferentiated (High grade)

Table 1

Thus, high grade tumors can not be easily distinguished from the surrounding healthy tissue with help of a scan. These are aggressive malignant tumors, which diffuse profusely to other parts of the body. On the other hand, low grade tumors have fixed boundaries and can be well differentiated from the healthy tissue [12].

Image Elastography

An elastogram is the mapping of material parameters (the Young's modulus, for example) in an anatomically meaningful image. The approaches to date have been to use conventional imaging methods to measure the mechanical response of tissue to mechanical stress. The resulting strains have been measured using ultrasound, CT, or MRI and the related elastic modulus has been computed from biomechanical models of tissues. In particular, the MR elastography method (MRE) using harmonic shear waves offers direct visualization and quantitative measurement of tissue displacements, high sensitivity to very small motions, a field of view unencumbered by acoustic window requirements, and the ability to obtain full three dimensional displacement information throughout a volume.

The process of generating elastograms using MRI is as follows. MR images are recorded while a vibrating plate placed on the skin propagates mechanical shear waves in the tissue. By putting the magnetic field in tune with the mechanical vibrations, the wavelengths of the propagating shear waves can be calculated and used in a biomechanical model of the tissue to further calculate the corresponding Young moduli. In particular, to find the stiffness of the brain tissue, vibrations can be applied either as vertical displacements to the base of the head, or as horizontal displacements to mouth via a bite block (Fig. 6, [19]). The Young's moduli of the white and gray matters are approximately 14.2kPa, and 5.3kPa, respectively. No values have been reported yet on the stiffness values of brain tumors.
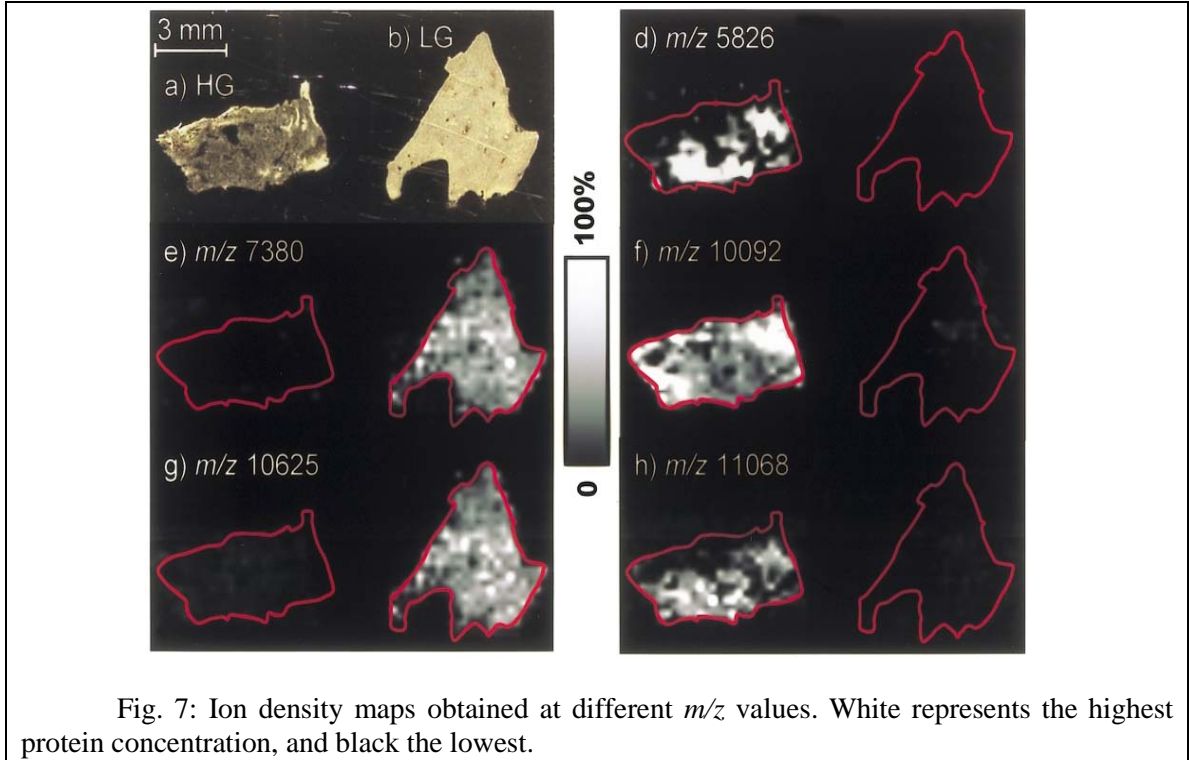
Fig. 6: MRE experiment setup (left and center) and a 2D elastogram (right) [19].
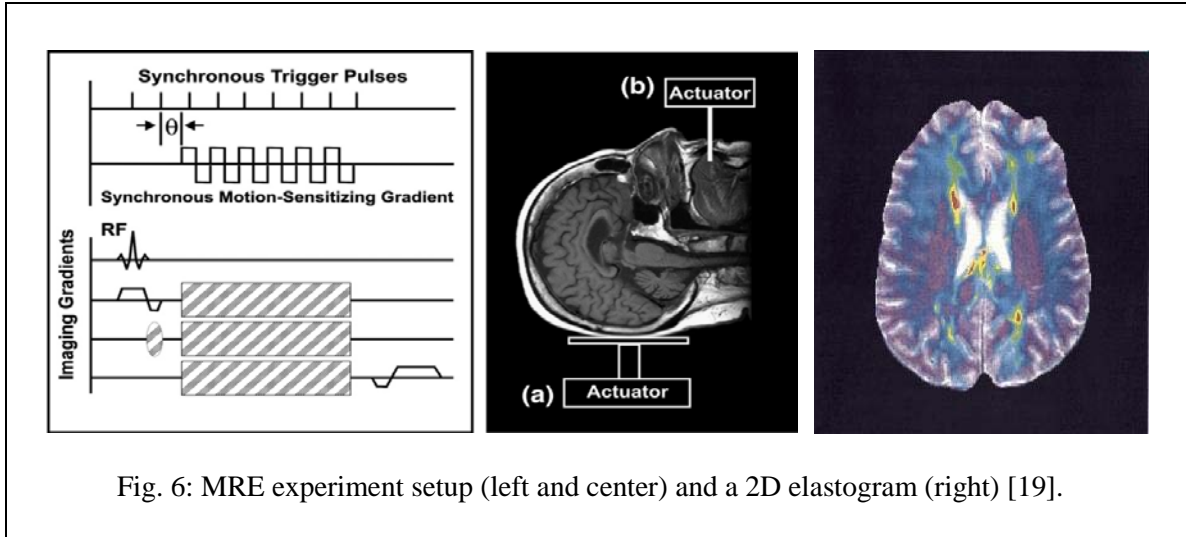
Chapter 3

Elastography-Mass Spectroscopy Model

In order to find Young's moduli of brain tumors that can be used to improve the non-invasive MRE method in the classification of tumors, we propose a novel biomechanical model based on image mass spectroscopy. Our aim is to relate the Young's modulus of gliomas to the concentration of certain proteins which have been shown to have different concentrations depending on the tumor's grade [10]. In Fig. 7 we reproduce some images from [10] of proteins concentrations found in low and high grade gliomas at different mass-to-charge ratios. In order to use the information provided by these image to calculate the Young's moduli of low and high grade gliomas, we make the following assumptions:

– the relative intensities of proteins given by IMS are proportional to the corresponding concentrations [20],

– the (apparent) Young's modulus of a tissue sample is proportional to the concentrations of proteins present in that tissue [13].

Fig. 7: Ion density maps obtained at different *m/z* values. White represents the highest protein concentration, and black the lowest.

We propose the following expression for the apparent Young's modulus E dependent on the concentrations $c_n, n = 1, 2...N$ of proteins given in Fig.7:

$$E = \sum_{n=1}^{N} c_n^{\alpha_n (m/z)}$$

The powers of the concentrations are assumed to depend on the corresponding mass to charge ratio (*m/z*) from Fig. 7 such that the apparent Young's modulus in the healthy tissue is

I). $\alpha_n = 1.8 = \text{constant}$

II). $\alpha_n = 1.6 + 1/(\ln(m/z)_n)$

approximately equal to the white matter value found by the MRE technique of 14.2 kPa [19]. We investigated the following two cases (the Matlab code is given in Appendix A):
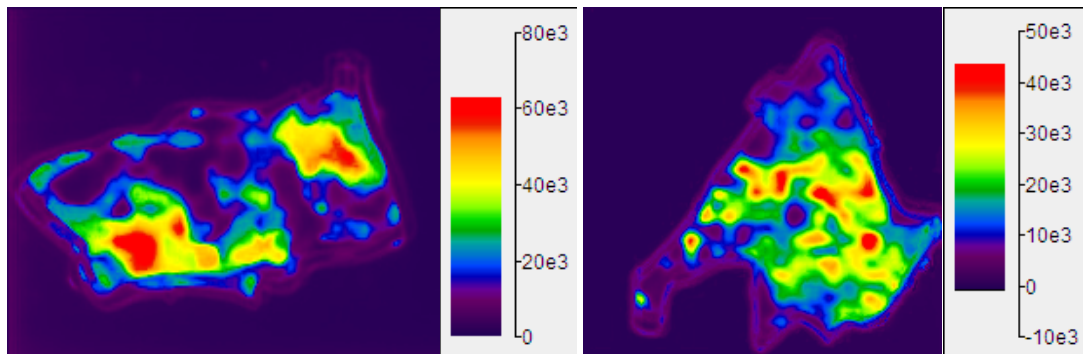

Fig. 8: Elastograms of high grade (left) and low grade (right) gliomas for case I.
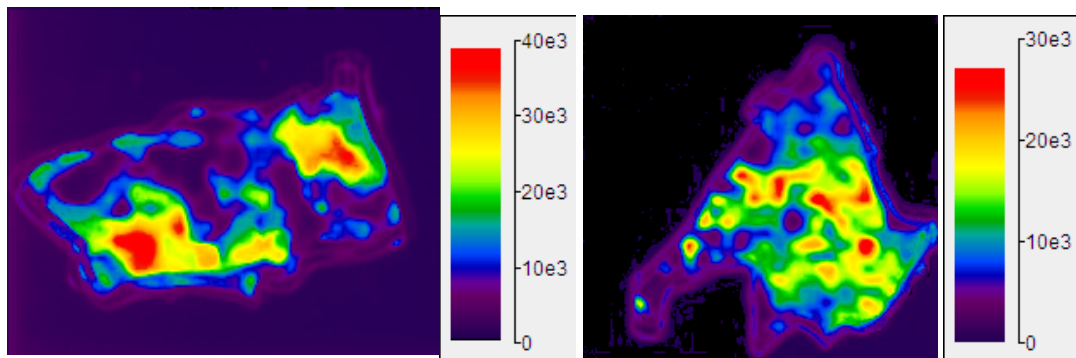

Fig. 9: Elastograms of high grade (left) and low grade (right) gliomas for case II.

From Figs. 8 and 9 we conclude that **high grade gliomas are at least 10kPa stiffer than low grade gliomas.** To the best of our knowledge, this is the first time when such a biomechanical model linking the stiffness of a tissue and the concentrations of proteins present in

the tissue and, more importantly, when such a clear differentiation between low and high grade gliomas has been established.

Chapter 4

Mechano-Growth Model

In this chapter we investigate the effect of mechanics on the growth of low and high grade gliomas. For simplicity we will consider the case of one-dimensional growth under applied uni-axial stretch λ (Fig.10). The tumor's growth is not caused by the applied stretch, it is assumed to happen independently of the mechanics.

Fig. 10: Schematic of the uni-axial stretch of a tissue with growing tumor.
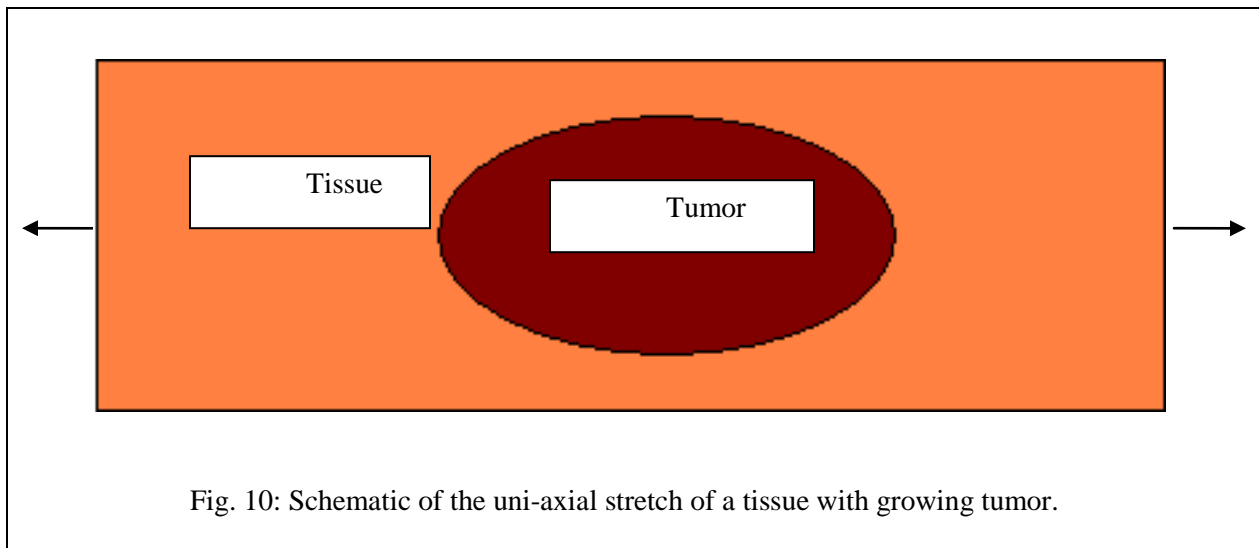
In order to make some progress in this challenging research area, we assume the growth to be volumetric and isotropic (the growth depends only on the time variable). As in [21], a

volumetric growth describes only geometric changes, the material points are dense during growth, and the intrinsic mechanical properties of the material do not change during growth. In addition, we assume for now that the tissue is an isotropic, homogeneous, linear elastic solid material.

If we denote by $F_d, G,$ and $F = F_d G^{-1}$ the deformation gradient of the applied uni-axial stretch, the growth tensor, and, respectively, the total deformation gradient (see Fig. 11 for more information), then the Cauchy stress tensor is given by Hooke's law:

$$\sigma = E\left(\frac{\lambda}{g(t)} - 1\right)$$

where E is the Young's modulus and $g(t)$ is the isotropic growth function.

Fig. 11: Kinematics of the coupled growth-deformation of a tumor.
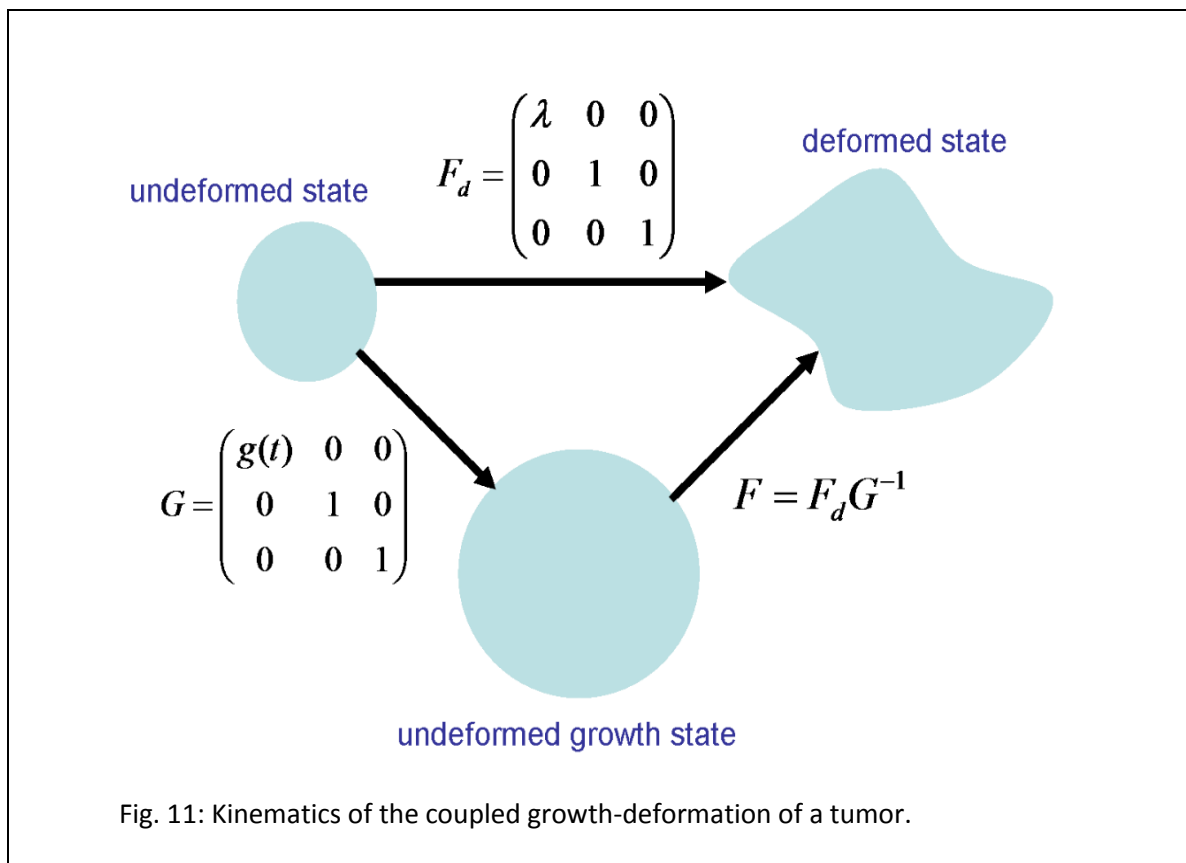
If we replace the above expression of the stress in the equation of growth proposed in [14], we obtain the following first order, nonlinear differential equation:

$$\frac{dg(t)}{dt} = \exp\left(\frac{\gamma E\left(\frac{\lambda}{g(t)}-1\right)}{k_B T}\right) g(t)$$

where T, k_B, γ are the absolute temperature, Boltzman constant, and, respectively, a parameter depending on the bio-chemical reactions involved in the growth process.

If we solve the linearized equation we obtain:

$$g(t) = \exp\left(\frac{\exp(\alpha E\lambda)}{\alpha E\lambda} - \frac{\exp(\alpha E\lambda)}{\alpha E\lambda}\exp(-\exp(\alpha E\lambda)\alpha E\lambda t)\right)$$

This solution is represented in Fig. 12 for different values of the stretch λ for low and high grade gliomas (the Matlab code used to generate these plots is given in Appendix A). We note that for small stretches $0 < \lambda \leq 1$ the growth of a low grade glioma appears to be as fast as that of a high grade glima. However, as the stretch increases and we approach the limits of validity of the linearity assumption, the high grade glioma increases much faster than the low grade glioma and both types of tumors will reach limiting sizes after which they will stop growing. These sizes are determined by the applied stretch.

Fig. 12: Growth functions for low (red) and high (blue) grade gliomas for different stretch values.
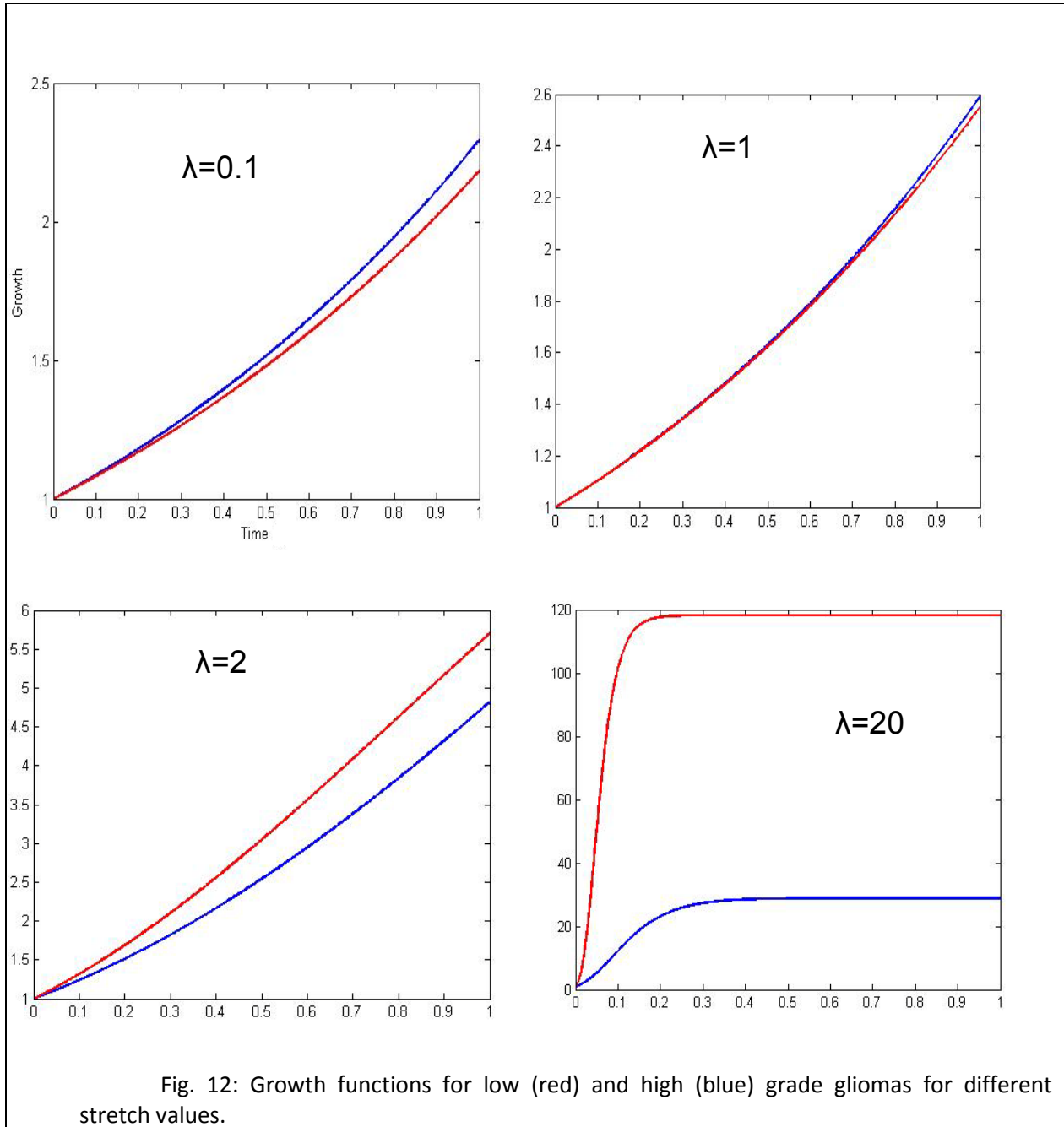
Chapter 5

Conclusion and Further Work

In this thesis we proposed two novel biomechanical models: one that estimates the Young's moduli of low and high grade gliomas based on the concentrations of proteins as given by image mass spectroscopy, and another model that predicts the growth behavior of these two types of gliomas under uni-axial stretch. Our first model showed that we can differentiate between low and high grade gliomas based on their (apparent) stiffness, a high grade being at least 10kPa harder than a low grade glioma. Such information can play an important role in the development of better, non-invasive diagnostic and treatment procedures based on image elastography.

Our mechano-growth model showed how an applied uni-axial stretch λ changed the growth of low and high grade gliomas. More precisely, when λ was less than 1, the growth of the low grade glioma was slightly higher than that of the high grade glioma, when it was closer to 1, both growth functions were identical, while when it became larger than 1, we found out that the high grade glioma had a steeper growth rthan the low grade glioma.

In our future work we plan to solve the fully non-linear equation of growth that we proposed in our mechano-growth model and to generalize this model in such a way that it will be able to predict when a low grade glioma turns into a high grade one. The model will be compared with another model that couples mechanics and growth proposed in [15].

References

1. Aebersold, R., and Goodlett, D. R. (2001). Mass spectrometry in proteomics. *Chem Rev* **101**, 269–95.

2. Russell, D. H., and Edmondson, R. D. (1997). High-resolution mass spectrometry and accurate mass measurements with emphasis on the characterization of peptides and proteins by matrix-assisted laser desorption/ionization time-of-flight mass spectrometry. *J Mass Spectrom* **32**, 263–76.

3. Cotter, R. J. (1999). The new time-of-flight mass spectrometry. *Anal Chem* **71**, 445A–51A.

4. Todd, P. J., Schhaaff, T. G., Chaurand, P., and Caprioli, R. M. (2001). Organic ion imaging of biological tissue with SIMS and MALDI. *J Mass Spectrom* **36**, 355–69.

5. Chaurand, P., and Caprioli, R. M. (2002). Direct profiling and imaging of peptides and proteins from mammalian cells and tissue sections by mass spectrometry. *Electrophoresis* **23**, 3125–35.

6. Chaurand, P., Schwartz, S. A., and Caprioli, R. M. (2002). Imaging mass spectrometry: a new tool to investigate the spatial organization of peptides and proteins in mammalian tissue sections. *Curr Opin Chem Biol* **6**, 676–81.

7. Chaurand, P., Schwartz, S. A., and Caprioli, R. M. (2004b). Profiling and imaging proteins in tissue sections by mass spectrometry. *Anal Chem* **76**, 86A–93A.

8. Quong, J. N., Knize, M. G., Kulp, K. S., Wu, K. J., (2004). Moleculespecific imaging analysis of carcinogens in breast cancer cells using time-of-flight secondary ion mass spectrometry. *Appl. Surface Sci.* **231**, 424–427.

9. Schwartz, S. A., Reyzer, M. L., and Caprioli, R. M. (2003). Direct tissue analysis using matrix-assisted laser desorption/ionization mass spectrometry: practical aspects of sample preparation. *J Mass Spectrom* **38**, 699–708.

10. Chaurand, Pierre, Sarah Schwartz, Michelle Reyzer, and Richard Caprioli (2005). Imaging Mass Spectroscopy: Principles and Potentials. *Toxicologic Pathology* **33**, 92-101

11. Tumor Grade: Q&A - National Cancer Institute.
http://www.cancer.gov/cancertopics/factsheet/Detection/tumor-grade

12. Tumor - Body, Process, Type, Characteristics, Cells, Surface, Part, Benign and Malignant Tumors, Medical Approaches.
http://www.scienceclarified.com/Ti-Vi/Tumor.html

13. Normand, Valery, Didier Lootens, and Pierre Aymard (2000). New Insight into Agarose Gel Mechanical Properties *Biomacromolecules*, *American Chemical Society* **1**, 730–738

14. Kim, Jin S., and Sean X. Sun (2009). Continuum Modeling of Forces in Growing Viscoelastic Cytoskeletal Networks. *Journal of Theoretical Biology* **256**, 596-606.

15. Clatz, Oliver, Maxime Sermesant, Pierre-Yves Bondiau, Hervé Delingette, Simon Warfield, Grégoire Malandain, and Nicholas Ayache (2005). Realistic Simulation of the 3D Growth of Brain Tumors in MR Images Coupling Diffusion with Biomechanical Deformation. *IEEE Trans Med Imaging.* **24**, 1334-346.

16. Alberts B., Johnson A., Lewis J., Raff M., Roberts K., Walter P., Molecular Biology of the Cell, Fifth Edition, 2007.

17. http://antoine.frostburg.edu/chem/senese/101/atoms/images/ms3.jpg

18. Seeley, Erin, and Richard Caprioli (2008). Imaging Mass Spectrometry: Towards Clinical Diagnostics, *PROTEOMICS - Clinical Applications* **2**, 1435-443.

19. Kruse S.A., Rose G.H., Glaser K.J., Manduca A., Felmlee J.P., Clifford R.J.Jr., Ehman R.L.(2008). Magnetic Resonance Elastography of the Brain, *NeuroImage* **39**, 231-237.

20. Hirabayashi A., Sakairi M., Koizumi H. (1994). Sonic Spray Ionization Method for Atmospheric Pressure Ionization Mass Spectroscopy, *Anal.Chem.* **66**, 4557-4559.

21. Chen Y.C., Hoger A. (2000). Constitutive Functions of Elastic Materials in Finite Growth and Deformation, *J.Elasticity* **59**, 175-193.

Appendix A

MATLAB Codes

```matlab
%%%%%%%%%%%%%%%%%%%%%%%%%%%%%
% This program builds elastograms (images of the Young modulus) at a certain mass-
%per-charge (m/z) ratio using images of mass spectroscopy.
%%%%%%%%%%%%%%%%%%%%%%%%%%%%%

m=imread('5826.jpg');
n=imread('7380.jpg');
o=imread('10625.jpg');
p=imread('10092.jpg');
q=imread('11068.jpg');

b=rgb2gray(m);
c=rgb2gray(n);
d=rgb2gray(o);
e=rgb2gray(p);
f=rgb2gray(q);

newb=double(b);
newc=double(c);
newd=double(d);
newe=double(e);
newf=double(f);

figure, imagesc(newb);

impixelinfo;


alpha_b=0.6+log(1/5826);
alpha_c=0.6+log(1/7380);
alpha_d=0.6+log(1/10625);
alpha_e=0.6+log(1/10092);
alpha_f=0.6+log(1/11068);

Young_Modulus=newb.^alpha_b+newc.^alpha_c+newd.^alpha_d+newe.^alpha_e+newf.^alpha_f;

figure, imagesc(Young_Modulus); %elastogram
```

```
%%%%%%%%%%%%%%%%%%%%%%%
%This program builds elastograms (images of the Young modulus) at
%a certain mass-per-charge (m/z) ratio using images of mass spectroscopy.
%%%%%%%%%%%%%%%%%%%%%%%

m=imread('5826.jpg');
n=imread('7380.jpg');
o=imread('10625.jpg');
p=imread('10092.jpg');
q=imread('11068.jpg');

b=rgb2gray(m);
c=rgb2gray(n);
d=rgb2gray(o);
e=rgb2gray(p);
f=rgb2gray(q);

newb=double(b);
newc=double(c);
newd=double(d);
newe=double(e);
newf=double(f);

figure, imagesc(newb);

impixelinfo;

alpha=0.6;

Young_Modulus=newb.^alpha+newc.^alpha+newd.^alpha+newe.^alpha+newf.^alpha;

figure, imagesc(Young_Modulus); %elastogram
```

```matlab
%%%%%%%%%%%%%%%%%%%%%
% This code is for the mechano-growth model.
%%%%%%%%%%%%%%%%%%%%%%

clear all
clc

K0=1;

gamma=1.3*10^(-26); %m^3
kB=1.3*10^(-23); %m^2*Kg/(s^2*K)
T=298; %K

alpha=gamma/(kB*T);

E_lg=30*10^(3); %Pa=Kg/(s^2*m); low grade
E_hg=40*10^3; %high grade

K_lg=K0*exp(-alpha*E_lg);
K_hg=K0*exp(-alpha*E_hg);


lambda=1;

beta_lg=K_lg*exp(alpha*E_lg*lambda);
beta_hg=K_hg*exp(alpha*E_hg*lambda);

t=0:0.001:1; %normalized time scale

%the growth functions are dimensionless

g_lg=exp(beta_lg/(alpha*E_lg*lambda).*(1-exp( beta_lg*alpha*E_lg*lambda.*t)));
g_hg=exp(beta_hg/(alpha*E_hg*lambda).*(1-exp(-beta_hg*alpha*E_hg*lambda.*t)));

plot(t, g_lg, 'b', t, g_hg, 'r', 'LineWidth', 2)
```

Academic Vita

Anthony J. Palocaren

1505 Anna Avenue   (412)-352-7040
West Mifflin, PA 15122   ajp5099@psu.edu

Education:

The Pennsylvania State University
Bachelor of Science, expected May 2010
Major: Engineering Science,
Schreyer Honors College

Experience:

Research in Micro-Turbo Machinery, May 2008-August 2008
Texas A&M University, College Station TX
- Analyzed conditions for failure of micro-endmills using 316L Stainless Steel.
- Simulated cutting conditions on micro-endmills using finite element analysis and SolidWorks COSMOS©.

Energy conservation study using thermal imaging camera, January08–March08
Pennsylvania State University, McKeesport PA
- Determine the loss of energy through the existing windows of the Frable building.
- Investigative analysis done using a thermal imaging camera provided by the Pennsylvania Technical Assistance Program (PennTAP).

Studied magnetic levitation with super conductors, June 2007-December 2007
Pennsylvania State University, McKeesport PA
- Built a model maglev train, as part of honors project, using super-conductors and electromagnets.

Organized West Mifflin Food Drive for Homeless/Poor, June 2005-March 2006
West Mifflin Area High School, West Mifflin PA
- In charge of organizing food drive, in conjunction with Boy Scouts of America, for the homeless.
- Collected 15,000 units of food and distributed to the poor and homeless in and around greater Pittsburgh.

Activities:

Member of US Army ROTC
Member of TAU BETA PI engineering honors society
Member of Penn State Army ROTC cadet recruiting team
Participant in intramural soccer league

Awards & Accomplishments:

Military Officers Association of America Medal of Honor
American Legion Scholastic Medal of Honor
Penn State Chancellors Circle of Honor
Penn State Faculty award for Best Engineering Student
Traina Memorial Scholarship for outstanding academics and community service
Penn State Minority Award and Scholarship for outstanding minority
Robert & Sandra Poole Schreyer Honors College Scholarship in Engineering.